DATA-DRIVEN MODELS FOR INFRASTRUCTURE CLIMATE-INDUCED DETERIORATION PREDICTION

By

Yasser Elleathy

B.Sc.

A Thesis

Submitted to the School of Graduate Studies

In Partial Fulfillment of the Requirements

For the Degree of

Master of Applied Science

McMaster University

MASTER OF APPLIED SCIENCE (2021) **McMaster University**

CIVIL ENGINEERING **Hamilton, Ontario**

Title: DATA-DRIVEN MODELS FOR INFRASTRUCTURE CLIMATE-INDUCED DETERIORATION PREDICTION

Author: **Yasser Elleathy, B.Sc. (Ain-Shams University).**

Supervisor: **Dr. Wael El-Dakhakhni, Professor, Department of Civil Engineering and the School of Computational Science and Engineering.**

Number of pages: vii, 36

Abstract:

Infrastructure deterioration has been attributed to insufficient maintenance budgets, lacking restoration strategies, deficient deterioration prediction techniques, and changing climatic conditions. Considering that the latter adds more challenges to the former, there has been a growing demand to develop and implement climate-informed infrastructure asset management strategies. However, quantifying the impact of the spatiotemporally varying climate metrics on infrastructure systems poses a serious challenge due to the associated complexities and relevant modelling uncertainties. As such, in lieu of complex physics-based simulations, the current study proposes a glass box data-driven framework for predicting infrastructure climate induced deterioration rates. The framework harnesses evolutionary computing, and specifically multigene genetic programming, to develop closed-form expressions that link infrastructure characteristics to relevant spatiotemporal climate indices and predict infrastructure deterioration rates. The framework consists of four steps: 1) data collection and preparation; 2) input integration; 3) feature selection; and 4) model development and result interpretation. To numerically demonstrate its utility, the proposed framework was applied to develop deterioration rate expressions of two different classes of concrete and steel bridges in Ontario, Canada. The developed predictive models reproduced the observed deterioration rate of both bridge classes with coefficient of determination (R^2) values of 0.912 and 0.924 for the training subsets and 0.817 and 0.909 for the testing subsets of the concrete and steel bridges, respectively. Attributed to its generic nature, the framework can be applied to other infrastructure systems, with available historical deterioration data, to devise relevant effective asset management strategies and infrastructure restoration standards under future climate scenarios.

Keywords: Asset Management, Bridge Condition Index, Climate Indices, Data-Driven Models, Deterioration Rate, Genetic Programming, Infrastructure, Multigene, Symbolic regression.

Acknowledgement:

I express my deepest thanks and pray to God for the blessings he gave me throughout my life and for empowering me with the ability to finish this thesis. I am eternally grateful to my mom, who dedicated her life to teaching me all the ethics and morals to be what I am today; God rest her soul. I express my gratitude to my lifetime sincere friend, who helped me a lot in my carrier and my academic research. I am extending my gratitude to my wife and kids for supporting me all the time and making things much easier in such hard times. Lastly, I want to thank my supervisor Dr. Wael El-Dakhakhni whose knowledge and innovative insight inspired me to finish this thesis.

Table of Content:

List of Figures:

List of Tables:

Notations:

C0: Biased Coefficient in Multigene Genetic Programming expression

C(i): Weighting Coefficient (i) in Multigene Genetic Programming expression

G_{max} = Maximum allowed number of genes in the expression

L_d = Deck length in m

N = Number of individuals in the generation population

n_s = Number of bridge spans

P_c = Crossover probability

P_m = Mutation probability

R^2: Coefficient of Determination

X_i = Feature number (i) in the selected subset

μ_i = the mean of the variable (i)

σ_i = the standard deviation of the variable (i)

$\hat{Y}$ = predicted output

List of Acronyms:

ADR: Average Deterioration Rate

AIC: Akaike Information Criterion

BCI: Bridge Condition Index

BIC: Bayesian Information Criteria

C.I. = Climate Indices

DDM: Data-Driven Models

GP: Genetic Programming

MGGP: Multigene Genetic Programming

MTO: Ministry of Transportation of Ontario

RMSE: Root Mean Square Error

S.D. Standard Deviation

1. INTRODUCTION

Infrastructure deterioration can be attributed to numerous natural and anthropogenic factors. The latter include insufficient design, improper materials, poor deterioration prediction models leading to deficient rehabilitation planning (Elmansouri et al., 2020; Mirza, 2006), and human activity contribution to climate change (Bastidas-Arteaga et al., 2013; Ring et al., 2012). On the other hand, natural factors include different forms of hazards such as hurricanes (Inkoom et al., 2021; Yang & Frangopol, 2020), floods (Sultana et al., 2018), sea level rise (Melchers, 2006) increased groundwater salinity (Cui et al., 2016), increased air chloride diffusion (Strauss et al., 2013), and elevated atmospheric carbon dioxide level (Stewart et al., 2011), as well as changes to ambient climate characteristics (e.g., precipitation, temperature) (C. M. Chang et al., 2021; Derrible et al., 2020). Greenhouse gas emission has resulted in major changes in climate patterns (Scheffran & Battaglini, 2011), subsequently resulting in weather extremes occurring more frequently (Rahmstorf & Coumou, 2011). Such extremes have significantly affected infrastructure health and deterioration rates negatively (Tari et al., 2015; Khelifa et al., 2013), highlighting the urgent need to develop effective infrastructure deterioration rate prediction models that explicitly account for climate characteristics (Jeong et al., 2017; Liu et al., 2020).

Most governments and municipalities adopt different infrastructure management systems to ensure infrastructure functionality and provide timely and adequate rehabilitation throughout their lifespan (Bolar et al., 2014; Assaad & El-adaway, 2020a). Infrastructure *reactive* management systems employ either numerical or categorical indicators that reflect the condition of the considered infrastructure following field inspections. Such indicators, in turn, are estimated based on safety, performance, monetary or integrated asset measures for different infrastructure components to quantify the infrastructure's overall condition (Y. Shen et al., 2019). However,

proactively, infrastructure condition should be also predicted over its remaining lifespan in order to devise effective asset management strategies. Several infrastructure deterioration modelling methodologies have therefore been developed to estimate infrastructure conditions over their lifespan deterministically (Zhang & Durango-Cohen, 2014), stochastically (Bu et al., 2013; M. Chang et al., 2019), or mechanistically (Lounis & Madanat, 2002; Nickless & Atadero, 2018).

Deterministic infrastructure deterioration models assume a monotonic relationship between infrastructure condition and influencing factors. Linear and nonlinear regression are the typical approaches used to develop such models; however, such approaches usually do not account for the complex-uncertain mechanisms of infrastructure deterioration. Stochastic infrastructure deterioration models aim at estimating the statistical behavior of the deterioration measures (e.g., infrastructure condition, time spent in a specific condition) such that the different sources of uncertainty inherent within the deterioration process are understood. The stationary Markov chain is most often applied to develop such deterioration models; however, a significant amount of infrastructure inspection data is typically required to ensure the stationarity assumption (Jiang et al., 1988; Jiang & Sinha, 1989). Therefore, the stationary Markov chain has been recently coupled with nonlinear and evolutionary optimization techniques to overcome the typical violation of such assumptions (Yosri et al., 2021; Bu et al., 2014; Wellalage et al., 2015). In contrast to deterministic and stochastic deterioration modelling methodologies, their mechanistic counterparts aim at predicting infrastructure conditions based on physical/chemical/functional phenomena contributing to deterioration. The availability of mathematical formulae describing such phenomena is thus essential to building such mechanistic (i.e., physics-based) infrastructure deterioration models.

Despite the substantial number of applications of deterministic, stochastic, and mechanistic modelling to estimate the temporal infrastructure condition, most former studies adopting such methodologies have not explicitly considered the climatic conditions' effect on the deterioration process throughout the infrastructure lifespan. The global climate change and its weather extremes present major challenges, to such assumptions, that are expected to remain persistent for the foreseeable future. This situation subsequently highlights the need to integrate relevant climate metrics within infrastructure deterioration models to inform effective climate adaptation strategies (Peng & Stewart, 2016; Stewart et al., 2012). Climate conditions can generally be characterized by temperature and precipitation indices (Sillmann & Roeckner, 2008). Approaches focused on integrating such spatiotemporal indices with infrastructure characteristics within multi physics-based simulations produce complex prediction models with low accuracy attributed to the numerous sources of uncertainty (Camacho, 2009; Underwood et al., 2020).

Data-driven models (DDM) present an efficient alternative to physics-based modelling of interacting systems (Zhou et al., 2020). In DDM, multiple inputs describing the characteristics of two or more systems (e.g., climate and infrastructure) are mathematically integrated to predict an output(s) of interest (e.g., infrastructure deterioration rate). It is also beneficial to consider DDM techniques that produce symbolic regression expressions (glass box) in lieu of typical black box techniques (e.g., deep learning) (Berardi et al., 2008; Cho, 2021). This will empower users to directly use the developed deterioration rate expressions without prior algorithm development knowledge. Such symbolic regressions can be achieved through parametric or nonparametric approaches, where classical regression (i.e., linear, and nonlinear) and artificial neural networks are examples of parametric DDM approaches that assume a fixed mathematical formula for the input-output relationship (Chukwu & Adepoju, 2012). Evolutionary computing techniques—a class of nonparametric DDM approaches, continuously evolve initial mathematical expressions

until the input-output relationships are sufficiently captured. Genetic Programming (GP) is one example of such techniques (Gondia et al., 2020) and is inspired by the concept of biological evolution proposed by Darwin (1859).

Using the exact resemblance with evolution theory, the application of the GP starts with a predefined number of randomly generated expressions (individuals). Depending on the expressions' ability to mimic the input-output relationship, individuals are either preserved or merged/changed in an attempt to create offspring with better performance. This process is repeated continuously until a prespecified termination criterion is satisfied. Due to its efficacy, DDM has been applied to simulate the infrastructure deterioration process (Yin et al., 2020; Ishida et al., 2021), with only few studies considered some basic climate characteristics (Piryonesi & El-Diraby, 2021).

The present study develops a framework using a climate based DDM to produce closed form expressions that can predict the infrastructure deterioration rates efficiently. The framework starts by collecting datasets representing the infrastructure's spatiotemporal and functional characteristics and associated climate indices. The temporal infrastructure conditions are subsequently converted to corresponding deterioration rate metrics, as described in detail later. A geospatial analysis is then carried out to link climate indices and infrastructure characteristics while representing climate indices by their corresponding statistical measures (e.g., means, standard deviation). Since the resulting integrated dataset (of the infrastructure-climate system) may include redundant information caused by interrelated parameters and noise introduced by irrelevant parameters, identifying, and applying an efficient feature selection procedure is thus key. Finally, a symbolic predictive model for the deterioration rate can be developed using DDM approaches, and the model feasibility, performance, and complexity can be subsequently analyzed.

2. FRAMEWORK ARCHITECTURE

Figure.1 illustrates the proposed framework which provides a standardized way to integrate the parameters describing the climate and infrastructure systems to develop a representative infrastructure deterioration rate expression. The framework encompasses four steps: (1) data collection and preparation; (2) input integration; (3) feature selection; and (4) model development and result interpretation. A detailed description of each of these steps is provided in the following sections.

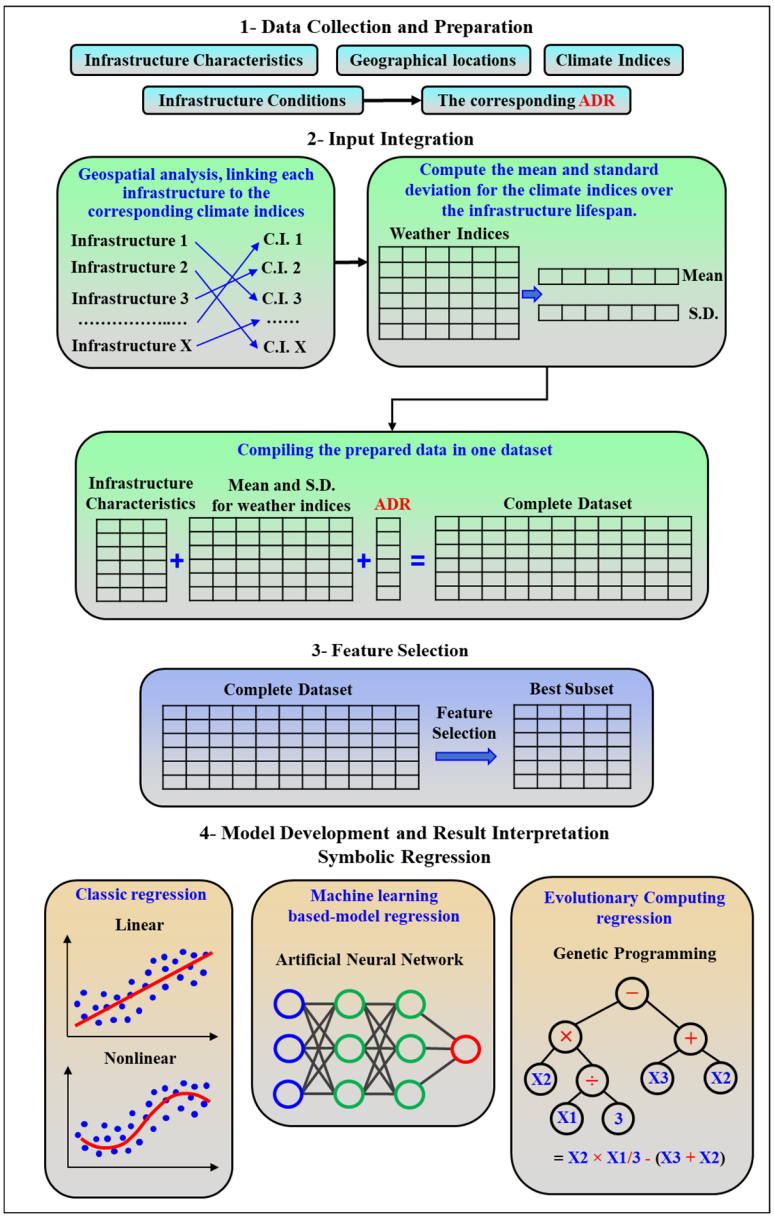

Fig. 1. Framework architecture

2.1. DATA COLLECTION AND PREPARATION

In this step, values of different infrastructure parameters that can affect the deterioration rate should be compiled. Such parameters may include material, geometry, safety, functionality, and location (latitude and longitude) data. Climate indices should also be collected at this step, where precipitation and temperature indices are typically used to describe the spatiotemporal climate conditions. The former set of indices can include the annual number of days with rainfall, snowfall, precipitation, consecutive dry days, and the quantity of pouring, whereas the latter set of indices can contain the annual number of hot, cold, and freezing days and nights, and the 5^{th} and 95^{th} percentiles of the maximum and minimum temperatures in the four seasons (Mekis & Vincent, 2008). Such indices are typically derived from daily precipitation and temperature records acquired from in-situ weather stations or from regional climate models calibrated using measurements from these stations (IPCC, 2021).

Finally, the infrastructure conditions of those existing in the study area need to be collected and subsequently used to estimate the corresponding deterioration rates. Infrastructure deterioration processes are typically nonlinear and nonstationary due to the complex nature of the deterioration mechanisms and the performance enhancement following minor or major interventions (i.e., rehabilitation). As such, successive records of infrastructure conditions can be used to calculate deterioration rates, and for simplification, the average can be used to represent the deterioration rate of the infrastructure over the considered time period assuming constant performance decline. When the aforementioned procedure is used, the overall average deterioration rate (ADR) of infrastructure reflects how it deteriorates over time, whereas a homogenization procedure should be performed for major rehabilitated infrastructures prior to and post-rehabilitation. It should also be noted that negative deterioration rate values may be

encountered when minor rehabilitation significantly improves the considered infrastructure performance or due to possible human data entry errors or subjectivity. Predictive DDM developed considering such (erroneous) observations might significantly underestimate the ADR value, and therefore such data points should be removed during the data collection and preparation step.

2.2. INPUT INTEGRATION

As the locations of infrastructures may not exactly coincide with weather stations where climate indices are evaluated, geospatial analysis is essential to identify the climate indices at each infrastructure location. Geospatial analysis has a wide range of applications, including interpolation and linkage. Interpolation includes assigning the infrastructure a weighted set of climate indices, where the weights can either be related to the distances between the infrastructure and surrounding weather stations (i.e., inverse distance weighted interpolation) or be calculated based on the variogram of climate indices (i.e., kriging interpolation) (Oliver & Webster, 1990). On the other hand, direct linkage refers to assigning each infrastructure the set of climate indices corresponding to the nearest weather station (De Smith et al., 2007). For simplicity, time series of climate indices that correspond to the infrastructure over its lifetime could be substituted by representative statistics (e.g., mean, standard deviation). After linking infrastructures to their corresponding climate indices statics, an integrated dataset can be prepared. Such dataset should contain: 1) input features, including the infrastructure characteristics and climate indices statics over the infrastructure lifetime; and 2) an output feature, which is the corresponding ADR.

2.3. FEATURE SELECTION

Feature selection is the process of identifying the best subset of nonredundant input features that can facilitate accurate prediction of the output of interest without: 1) sharing/replicating the same information (i.e., due to interdependence); 2) producing biased output; or 3) unnecessarily increasing the model complexity (Alabdulwahab & Moon, 2020). Several feature selection techniques have been developed, and can generally be classified under Filters, Wrappers, and Embedded techniques.

Filters are the simplest and most straightforward feature selection techniques, in which the strength of the relationship between inputs and input-output pairs are evaluated. Highly correlated inputs are subsequently replaced by a single representative one, and those of a lower correlation with the output of interest are eliminated. As such, filter-based feature selection techniques necessitate identifying a correlation measure (e.g., Pearson's correlation coefficient, Chi-squared) along with an input elimination threshold. (Duch, 2006).

Wrapper techniques, in contrast, rely on iteratively developing a predictive models based on different subsets of input features. When wrapper techniques are applied, the model performance is evaluated based on an error estimator (e.g., root mean squared error (RMSE), Akaike Information Criterion (AIC)) or a penalized error (e.g., Bayesian Information Criteria (BIC)). The optimal subset of input features is that produces the highest model performance. Examples of wrapper-based feature selection techniques include: 1) the forward stepwise variable selection, in which an initial model is developed based on a single input and iteratively adding more features until the model with the best performance is identified; 2) the backward stepwise variable elimination, in which the initial model is developed based on the full set of inputs and subsequently removing those with lower impacts on the model performance; 3) the stepwise regression, in which

both forward and backward stepwise methods are integrated; and, 4) genetic algorithms, in which a population of models is built based on different subsets of input features and subsequently evolve over iterations to identify more superior models. It should be emphasized that wrapper feature selection techniques typically result in more accurate models compared to those developed based on filter approaches; however, their applications are most often computationally demanding (Pistore et al., 2019).

An embedded feature selection technique allows the iterative choice of input features that significantly boost performance of the resulting model, albeit at a lower computational cost (Peralta & Soto, 2014). Examples of modelling approaches with embedded feature selection include the random forest, and GP. It should be emphasized that when a DDM approach with a built-in (i.e., embedded) feature selection technique is employed, the use of an external feature selection technique (i.e., filters and wrappers) should be avoided (Babatunde et al., 2014).

2.4. Model Development and Result Interpretation

After selecting the input subset that significantly influence the infrastructure deterioration rate, several DDM approaches can be employed to develop the ADR symbolic prediction model. These approaches include classical regression, supervised machine learning, and evolutionary computing techniques. Classical regression techniques aim at combining input features either linearly or nonlinearly. Coefficients typically exist within the model structure to reflect the contribution of each input feature to the model output, and their values are most often calculated based on least squared analyses. However, the development of classical regression models, particularly those linear ones, requires a monotonic relationship between each input-output pair and also necessitate the model errors to be normal and independent (Myers & Myers, 1990). Supervised machine learning techniques, such as artificial neural networks, represent more efficient alternatives to

classical regression techniques. Such techniques typically employ a linear-nonlinear model structure to capture complex input-output relationships. Model coefficients (weights) are iteratively adjusted through a backpropagation algorithm to minimize the difference between actual and estimated outputs. It is worth noting that extracting underlying symbolic expression from the artificial neural networks model is neither an easy nor a straightforward procedure (Taha & Ghosh, 1999). It also should be highlighted that both classical regression analysis and supervised machine learning techniques employ a predefined fixed model structure which restricts the developed model applicability (Cuevas et al., 2002; Yegnanarayana, 2009).

On the other hand, the more powerful evolutionary computing techniques can efficiently uncover complex input-output relationships through an adapted model structure (Gondia et al., 2020). Such techniques typically employ specific operations that prevent the solution from being trapped in local opima. GP is an example of evolutionary computing techniques used for predictive model development and can be adopted in a single- or multi-gene fashion. The application of GP starts by defining the operands and operation functions (Fig. 2), and subsequently develop an initial set of suggested solutions (i.e., initial population). Each solution witihn the population is typically referred to as an individual (expression) and represents a candidate mathematical relationship between the input and output features. Individuals are represented by variable-length tree-like structures, where an operation function is used as a root node and operands typically exist at terminal nodes (Fig. 2). A fitness value is subsequently assigned to each individual to reflect its suitability to replicate the actual output. Such value can be calculated based on an error estimator (e.g., RMSE), strength quantifier (e.g., R^2) of the relationship between the actual and predictied output, model performance cretieria (e.g., BIC), or a cost function that combines two or more measures. New individuals are continously reproduced over generations from precursors through

the application of: 1) elitism, where individuals with higher fitness are copied to the next generation; 2) crossover, where parts of two selected individuals are randomly shuffeled to produce two new offspring individuals (Fig. 3a); and 3) mutation, where part of a single individual is randomly changed (Fig. 3b). The most common selection methods used in this step are the tournament and roulette wheel methods. When a tournament selection is applied, a number of individuals (competitors) is chosen randomly and the competitor with the highest fitness value is selected for crossover or mutation. On the other hand, when the roulette wheel selection method is adopted, each individual is assigned a selection probability depending on its fitness value. Individuals are subsequently selected randomly from the entire population based on such probability (Chudasama et al., 2011).

It should be noted that elitism is typically applied to preserve high quality individuals over generations, whereas crossover and mutation are applied to increase the diversity within the remaining individuals such that their performance is enhanced over multiple generations. The reproduction process continues until a termination cretrion is sutisfied. Such certerion my be a specific number of generations, fitness value, computation time, or a combination of such metrics. Fig. 4 shows the typical steps followed when GP is applied. A detailed description of each of these steps is provided in the study by Koza (1994).

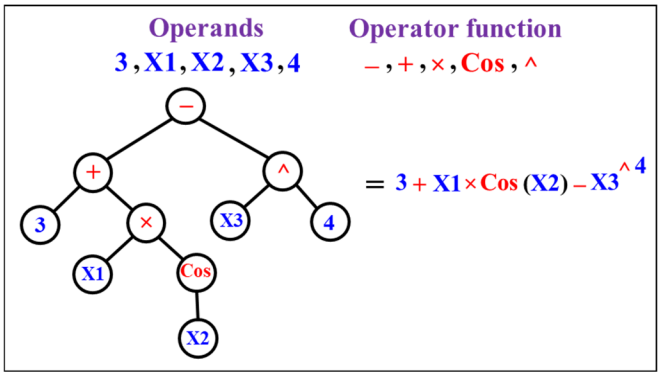

Fig. 2. Tree-like structure of individuals within the GP procedure

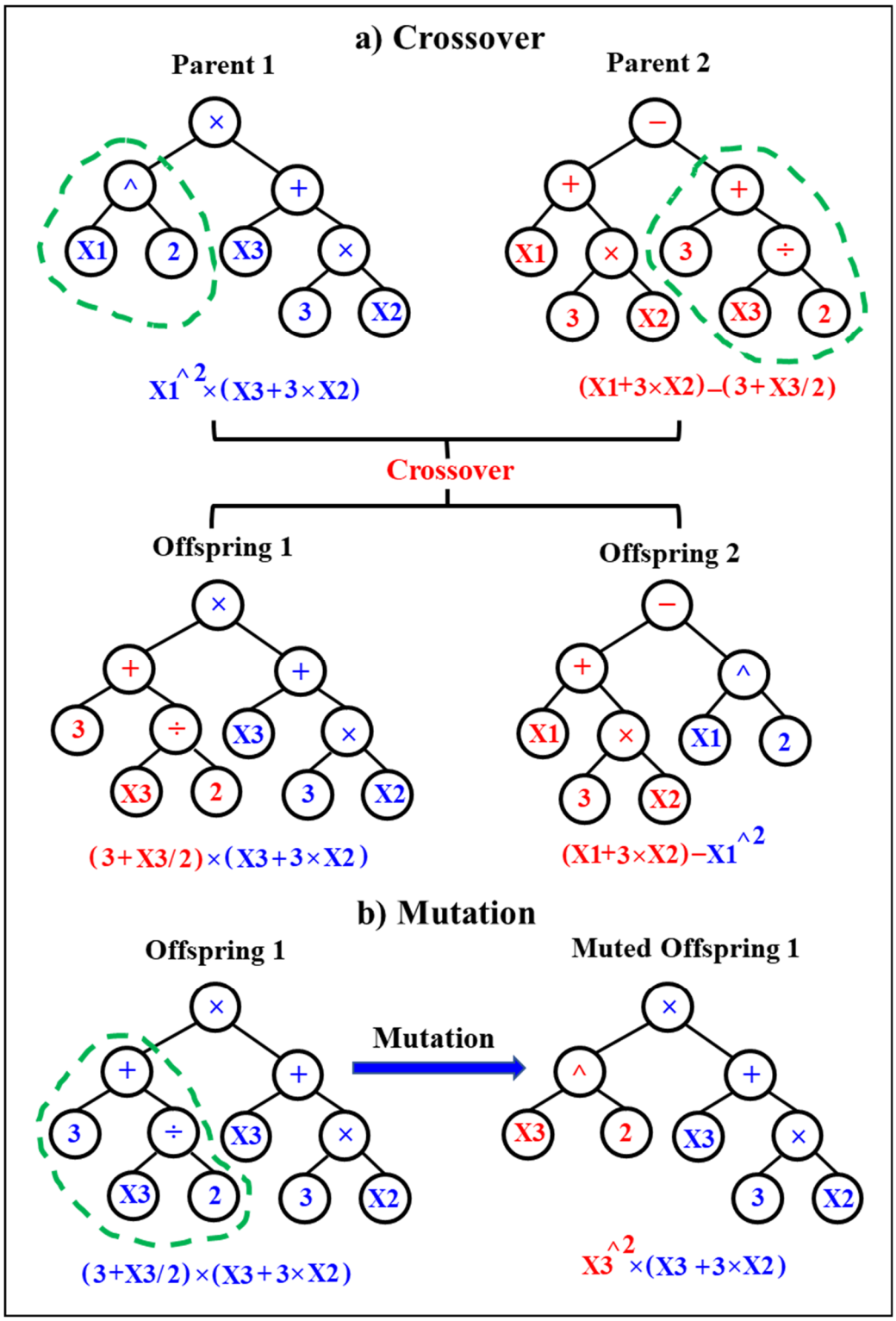

Fig. 3. Schematics of crossover and mutation

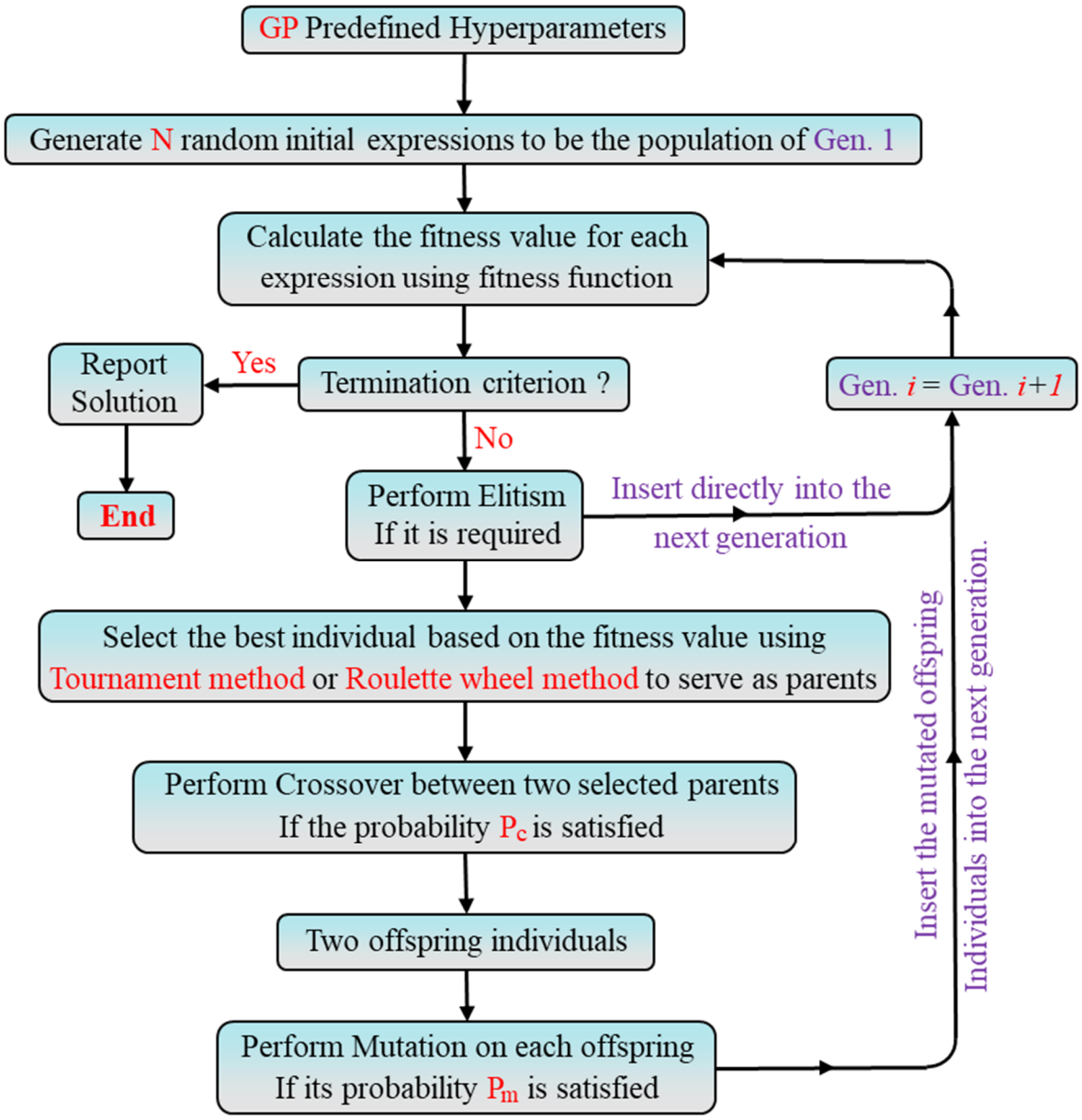

Fig. 4. GP application flowchart

Although the application of GP has proven to produce accurate predictive models in different fields (Grosman & Lewin, 2002; J. Shen & Jimenez, 2018), GP most often result in exceptionally complex mathematical expressions particularly when the number of input features is significantly large. It is thus more effective to apply GP in a *multigene* fashion, where low-depth (i.e., flat) non-linear individuals are combined within a linear regression model (Gandomi & Alavi,

2012). Fig. 5 shows an example of a mathematical expression developed based on the application of the multigene genetic programming (MGGP). In such example, the final mathematical model is the summation of a bias coefficient (i.e., C0) and two flat genes (trees 1 and 2), each of which is multiplied by a weighting coefficient (C1 and C2, respectively). These coefficients are evaluated to minimize the linear least-squares values between the predicted output ($\hat{Y}$) and the actual output. The MGGP thus merges the ability of the classical linear regression and the power of capturing the non-linearity without predefining a model structure. It should be noted that models developed using MGGP usually outperform those resulted from the application of the standard GP for the same inputs and outputs (Mehr & Safari, 2020). In addition, the application of MGGP provides more control over the model complexity compared to that when standard GP is applied. Expressional complexity is a measure of the complexity of a mathematical expression and is typically used to differentiate between flat and deep trees (Le et al., 2016). For example, if two trees have the same number of nodes, the flatter one has lower expressional complexity compared to the deeper one. A Pareto selection method is typically applied to choose a less complex solution as such approach considers both the fitness and complexity of the model rather than the model fitness only (Ekart & Nemeth, 2001).

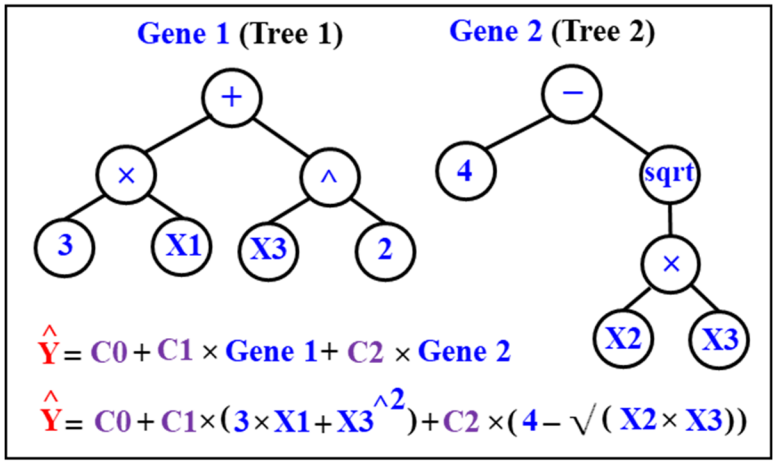

Fig. 5. An example of MGGP-generated expression

When the MGGP is employed, a random number of trees between 1 and a predefined number G_{max} is allocated to each individual within the initial population. Higher values of G_{max} increases the likelihood of capturing more non-linear interrelationships between inputs and outputs. However, such higher values of G_{max} facilitates the occurrence of horizontal bloat. The horizontal bloat is defined as the development of a complex model that capture the input-output relationship efficiently during training, but this complexity result in no appreciable enhancement in the model prediction performance (Gandomi et al., 2016). It should be noted that the choice of the population size is crucial when using the MGGP as it controls the convergence rate, individual quality, and, therefore, the final solution. A large population size increases the likelihood of obtaining an optimal solution at earlier generations (Rylander & Gotshall, 2002); however, individual diversity may intensify across the population such that rapid convergence cannot be achieved (Koljonen & Alander, 2006). It should be also noted that using a two-point high-level crossover is preferred to acquire new trees within each individual (Braik, 2021), as shown in Fig. 6.

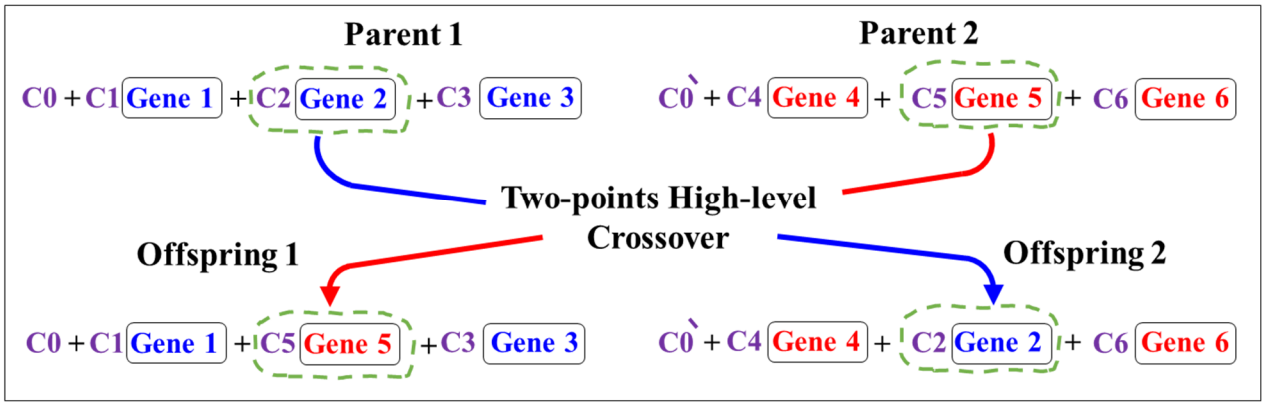

Fig. 6. Two-point high-level crossover procedure

3. DEMONSTRATION APPLICATION

To demonstrate its utility, the proposed framework is applied to develop a predictive model for the deterioration rate of highway bridges, as are key infrastructure susceptible to climate induced deterioration in North America (ASCE, 2009). In this respect predictive models developed based on the proposed framework can: 1) aid designers and practitioners to efficiently choose the bridge material, geometry, and structural system that allow the bridge to deteriorate slowly under both loading and climate conditions; and 2) help decision- and policymakers to prepare efficient management guidelines for bridges under climate change.

3.1. DATASET

The present study employs the bridge inventory database of the Ministry of Transportation of Ontario (MTO) and relevant climate indices to develop a closed form predictive expression for bridge ADR in the province of Ontario, Canada considering the climate impacts. The bridge inventory dataset contains the year of the construction, material-, geographical-, geometric-, and structural characteristics as well as inspection scores between the year 2000 and 2017 for 1,250 non-rehabilitated bridges made of concrete or steel in the province of Ontario. Inspection scores are reported in terms of a bridge condition index (BCI) that represents the bridge asset value compared to the corresponding replacement cost at the time of inspection (Stevens et al., 2020; Alzoor et al., 2021). Such measure reflects the overall bridge condition and inherently combines the conditions of the different components of the bridge. The BCI values range is between 0 and 100, where a large value indicates a higher bridge asset value and thus reflects a lower possibility of replacement.

Climate indices considered in the present study include 10 precipitation and 30 temperature indices (Table 1) acquired from 59 and 48 weather stations, respectively, across the province of Ontario. Such indices were calculated based on homogenized daily precipitation and temperature and provided at an annual basis for the time period between 1900 to 2016. Precipitation indices include the number of days with different precipitation forms (e.g., rainfall, snow), as well as the 1-day precipitation intensity. On the other hand, temperature indices are grouped into two sets: A and B. Set A contains indices for the number of days with a specific temperature, whereas set B encompasses the 5^{th} and 95^{th} percentiles of the maximum and minimum temperature of each season (i.e., winter, spring, summer, and fall) (Canadian Climate Data and Scenarios, 2019).

Table 1: Climate indices employed along with their definitions

Classification	Index	Definition
Precipitation	ndr	Number of days from January to December with rain ≥ 1 mm
	nds	Number of days from July to June with snow ≥ 1 mm
	ndp	Number of days from January to December with precipitation ≥ 1 mm
	h1r	Number of days from January to December with rain > 90th percentile
	h1s	Number of days from July to June with snow > 90th percentile
	h1p	Number of days from January to December with precipitation > 90th percentile
	x1r	Highest 1-day rain from January to December
	x1s	Highest 1-day snow from July to June
	x1p	Highest 1-day precipitation from January to December
	mcdd	Max number of days from January to December with precipitation < 1 mm
Temperature set (A)	sd	Number of days from January to December with maximum temperature > 25°C
	hd	Number of days from January to December with maximum temperature > 30°C
	tn1	Number of days from January to December with minimum temperature > 20°C
	tn2	Number of days from January to December with minimum temperature > 22°C
	fd	Number of days from July to June with minimum temperature ≤ 0°C
	cfd	Max number of consecutive days from July to June with minimum temperature ≤ 0°C
	id	Number of days from July to June with maximum temperature ≤ 0°C
	ft1	Number of days with minimum temperature ≤ 0°C and maximum temperature > 0°C
	ft2	Number of days from January to April with minimum temperature ≤ 0°C & maximum temperature > 0°C
	gdd5	Sum of degrees from January to December with mean temperature > 5°C
	cdd	Sum of degrees from January to December with mean temperature < 18°C
	hdd	Sum of degrees from January to December with mean temperature > 18°C
	FFS	Maximum number of consecutive days from January to December with minimum temperature > 0°C
	GS	start when mean temperature > 5°C for 6 days and end when mean temperature < 5°C for 6 days from Marsh to November
Temperature set (B)	WinTx05	Winter 5th percentile of maximum temperature from December to February
	WinTx95	Winter 95th percentile of maximum temperature from December to February
	WinTn05	Winter 5th percentile of minimum temperature from December to February
	WinTn95	Winter 95th percentile of minimum temperature from December to February
	SprTx05	Spring 5th percentile of maximum temperature from March to May
	SprTx95	Spring 95th percentile of maximum temperature from March to May
	SprTn05	Spring 5th percentile of minimum temperature from March to May
	SprTn95	Spring 95th percentile of minimum temperature from March to May
	SumTx05	Summer 5th percentile of maximum temperature from June to August
	SumTx95	Summer 95th percentile of maximum temperature from June to August
	SumTn05	Summer 5th percentile of minimum temperature from June to August
	SumTn95	Summer 95th percentile of minimum temperature from June to August
	AutTx05	Autumn 5th percentile of maximum temperature from September to November
	AutTx95	Autumn 95th percentile of maximum temperature from September to November
	AutTn05	Autumn 5th percentile of minimum temperature from September to November
	AutTn95	Autumn 95th percentile of minimum temperature from September to November

3.2. FRAMEWORK IMPLEMENTATION

3.2.1. DATA COLLECTION AND PREPARATION

Only bridges inspected more than one time between years 2000 and 2017 are considered in the present study as the bridge ADR can not be calculated from a single BCI value. The BCI of each of the considered bridges is converted into a corresponding ADR value, as described earlier. Fig. 7 shows the number of bridges constructed using different structural system and materials, as well as the corresponding deterioration rate.

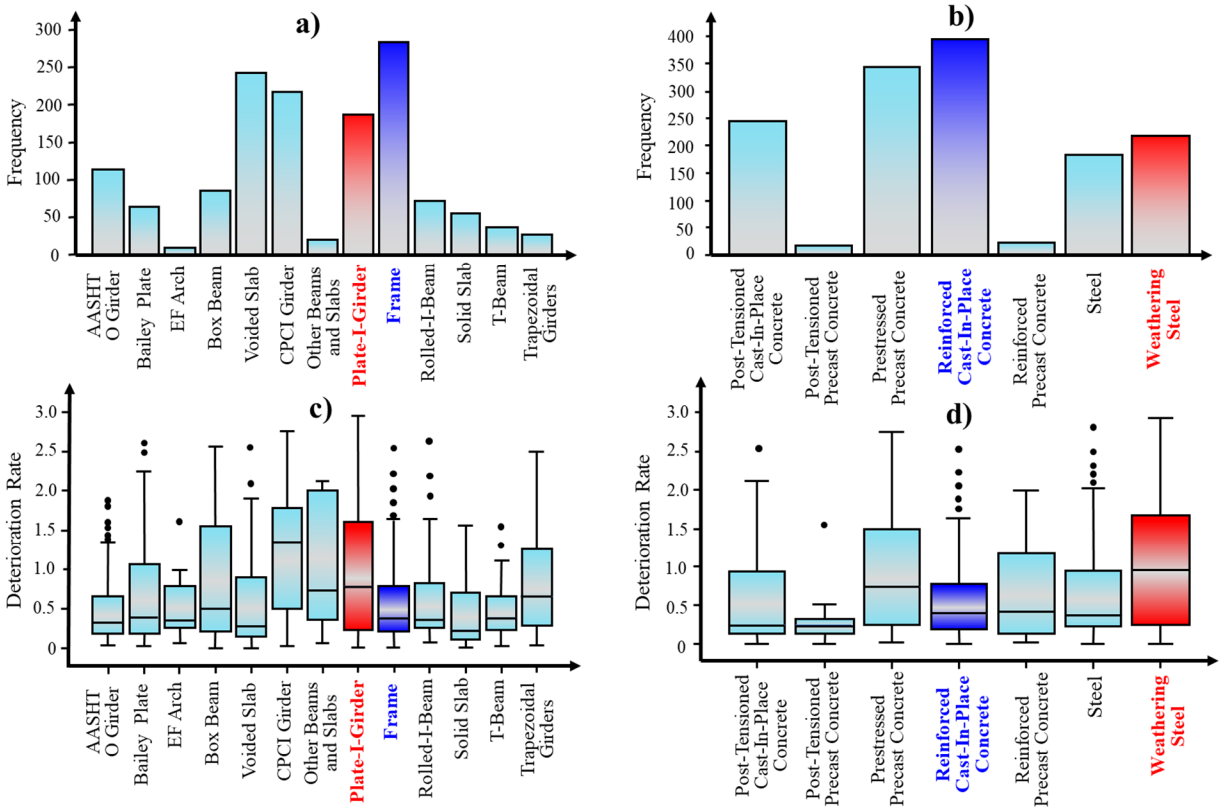

Fig. 7. Histogram of (a) a specific structural system and of (b) a specific construction material, and plot boxes of the deterioration rate grouped based on (c) the structural system and (d) the construction material

As can be revealed from Figs. 7a and 7b, the cast-in-place reinforced concrete frame bridges (in blue) represent a major portion of the bridges in the province of Ontario. In addition, weathering steel plate-I-girder bridges (in red) were observed to have the major portion of steel bridges in Ontario and a high deterioration rate compared to most other bridge types (Fig. 7c and 7d). As such, the present model demonstration application adopts the proposed framework to estimate the ADR of cast-in-place concrete frame and weathering steel plate-I-girder bridges only. After removing those with ADR outliers, the number of bridges within the two classes is 212 and 68, respectively. Geometric features considered for each bridge include the number of spans, longest span, deck length, and total width. Fig. 8 shows the histograms of these geometric features for the concrete and steel bridges considered in this demonstration application.

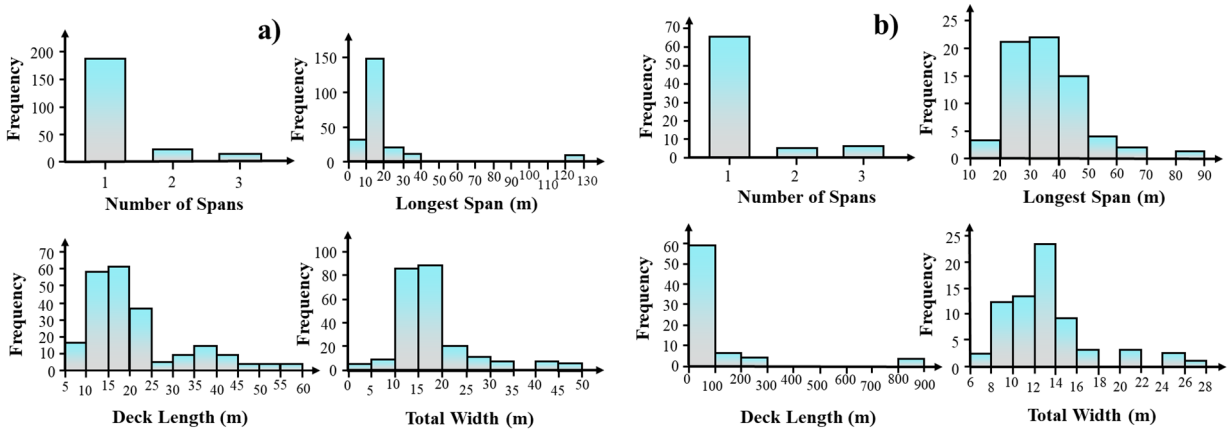

Fig. 8. Histograms of the geometric features (i.e., the number of spans, longest span, deck length, and total width) of the (a) concrete bridges and (b) steel bridges considered in the demonstration application

3.2.2. INPUT INTEGRATION

The purpose of this step is to prepare an integrated set of inputs that include geometric characteristics of bridges and climate indices at the bridge location. Figure 9 shows the location of the considered concrete and steel bridges as well as those of the considered weather stations. Considering the proximity of the bridges to related weather stations, climate indices are assigned to each bridge based on the nearest weather station (i.e., direct linkage) using the geodesic distance rather than interpolation.

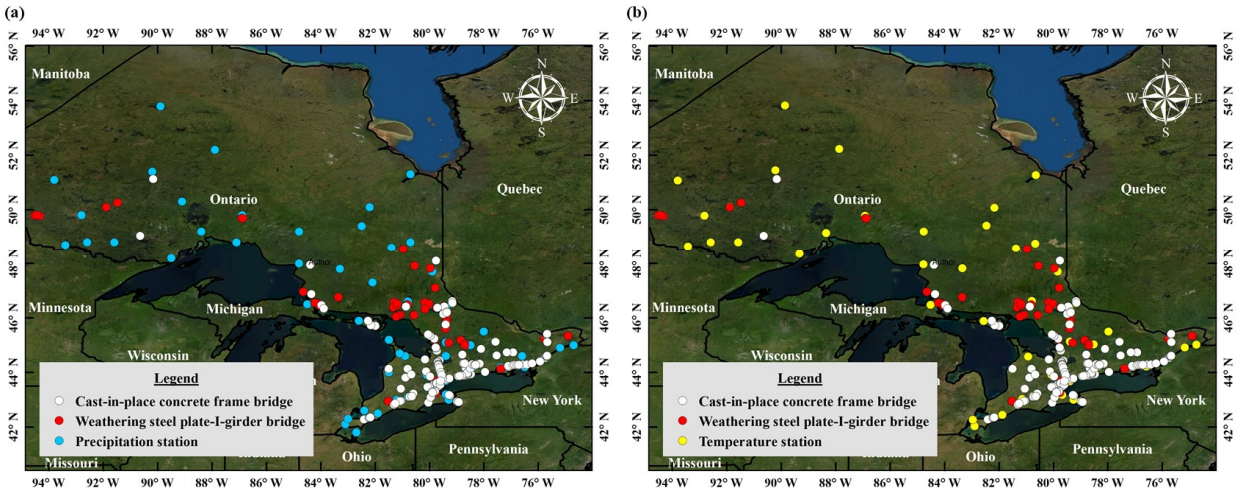

Fig. 9. The location of concrete and steel bridges considered in the demonstration application with respect to available (a) precipitation and (b) temperature stations in the province of Ontario

After linking each bridge to the nearest weather station, aggregate metrics (i.e., mean and standard deviation) for the precipitation and temperature indices are calculated to reflect the climate variability that affected each bridge over its lifetime. By calculating the mean and the standard deviation of each climate index, the integrated input dataset includes four bridges' geometric characteristics, 20 metrics for the precipitation indices, and 60 metrics for the temperature indices, all defined for each bridge within the considered dataset.

3.2.3. FEATURE SELECTION

In this demonstration application, the MGGP is used to uncover the complex relationship between the 84 input features and the corresponding ADR. Since the MGGP can internally select the input features most important for estimating the output, there is no need to use an external feature selection approach (i.e., filters or wrappers) as explained earlier.

3.2.4. MODEL DEVELOPMENT AND RESULT ANALYSIS

In this study, the MGGP was applied using the MATLAB© toolbox, GPTIPS, developed by Searson et al. (2010). The MGGP hyperparameters defined for the concrete and steel bridges are shown in (Table 2). These hyperparameters are defined through a trial-and-error procedure in order to obtain an optimal solution at a reasonable computational cost. The fitness function considered is the RMSE, with the aim of minimizing its value. As the absolute minimum of the RMSE cannot be easily achieved (i.e., RMSE = 0), a relatively higher fitness value is allowed in the present study. For each of the considered bridge classes, around 75% of the dataset were used for the model development (i.e., training) whereas the remaining 25 % of the data were kept for testing the obtained model.

Table 2: The employed MGGP procedure hyperparameters

	Cast-in-place Concrete Frame Bridges	Weathering Steel Plate-I-Girder Bridges
Operands	All the independent variables	
Operation functions	plus, minus, multiply, divide, square root, and power	
Population size	10,000	
Tree depth	3	
Max. number of genes G_{max}	6	5
Ratio of elite individuals	0.05	0.1
Crossover probability	0.7	0.85
Mutation probability	0.15	0.05
Termination criterion	Fitness value ≤ 0.03, or the number of generations = 250	

Figures 10a and 10b show the RMSE for the individuals within each generation for the concrete and steel bridges, respectively. The mean RMSE values were nearly constant after 100 generations for both bridge types, justifying the choice of 250 as the maximum number of generations (Table 2). The RMSE values of the best individual within the last generation were 0.14 and 0.21 for the training data and 0.16 and 0.25 for the test data for the concrete and steel bridges, respectively. Further investigations of the individuals within the final population showed that a less complex individual with a relatively higher R^2 (proposals P1 and P2) can still be used to efficiently estimate the ADR of both bridge classes as shown in (Fig. 10c and 10d). Accordingly, the individuals' proposals P1 (Fig. 10c) and P2 (Fig. 10d) were chosen as the near optimal ADR expressions for the concrete and steel bridges, respectively.

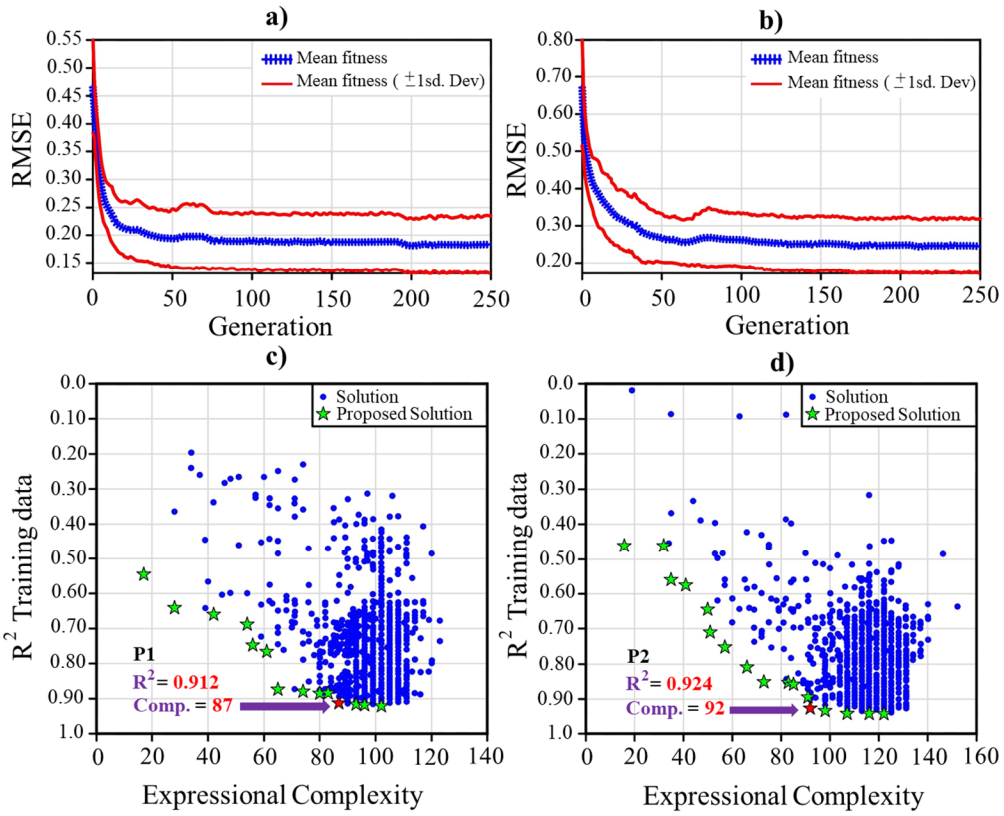

Fig. 10. The individuals mean RMSE value in each generation for (a) the concrete bridges and (b) steel bridges, as well the relation between the expression complexity and R^2 for individuals in the final population in case of (c) concrete bridges and (d) steel bridges

The mathematical representation of the proposal P1 for the concrete bridges and proposal P2 for the steel bridges are shown in Equations 1 and 2, respectively:

$$\begin{aligned} ADR = 1.75 &- \frac{0.08 \times \sigma_{ft2} \times \sigma_{WinTx95} \times \sigma_{WinTn05}}{\mu_{h1p}} + \frac{0.53 \times \mu_{AutTx05}}{\sigma_{WinTx95}} \\ &+ 0.01 \times \left(\mu_{h1p} + \frac{\mu_{fd}}{\sigma_{SumTx95}}\right) - 0.23 \times \left(\mu_{h1r} + \frac{\sigma_{SumTn95}}{0.66}\right) \\ &+ 0.0004 \times \frac{\mu_{hdd} + L_d}{\sqrt{\mu_{SumTn05}}} \\ &- 0.0044 \times (\mu_{h1r} + \sigma_{ft2} \times \mu_{mcdd} \times \sigma_{SumTx05}) \end{aligned} \quad (1)$$

$$\begin{aligned} ADR = 7.78 &- 0.0001 \times \mu_{cfd} \times \sigma_{WinTx05} \times \sigma_{WinTn05} \times (1.2188 + \sigma_{SumTn95} + \sigma_{ndr}) \\ &+ 0.0924 \times \mu_{h1s} - 0.0001 \times \sigma_{WinTx95} \times \mu_{ndr} \times (\sigma_{mcdd} + \sigma_{ndr} + \sigma_{WinTx05}) \\ &- 0.0007 \times \sigma_{WinTn05} \times \mu_{x1r} \times \sigma_{SumTn05} \times (\mu_{mcdd} + \sigma_{WinTn05} + \mu_{AutTx05}) \\ &\times (n_s + \mu_{SumTx95} + \sigma_{ndr}) \\ &- 0.064 \times (1.11 \times \sigma_{GS} + \sigma_{FFS} + \mu_{mcdd} + \sigma_{x1p}) \end{aligned} \quad (2)$$

where L_d is the deck length in m and n_s is the number of bridge spans.

The MGGP-based expressions shown in Eqns. 1 and 2 sufficiently reproduced the actual ADR of the concrete (R^2 = 0.912 and RMSE = 0.14 for the training subset; and R^2 = 0.817 and RMSE = 0.16 for the testing subset) and steel (R^2 = 0.924 and RMSE = 0.21 for the training subset; and R^2 = 0.909 and RMSE = 0.25 for the testing subset) bridges (Fig. 11), which supports the accuracy and generalizability of the two models.

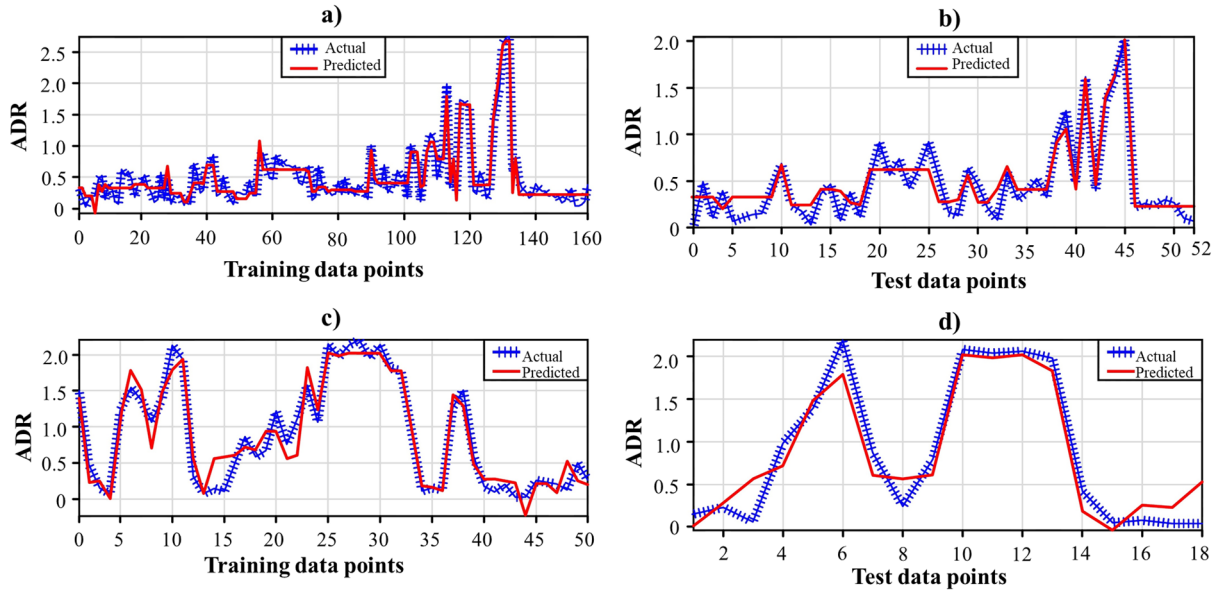

Fig. 11. A comparison between the actual and predicted ADR values for the (a) training and (b) testing subsets of the concrete bridges (proposal P1), and for the (c) training and (d) testing subsets of the steel bridges (proposal P2)

To further investigate the relationship between input-output pairs, the mean Shapely value was estimated for each of the independent variables in Eqns. 1 and 2 based on the methodology described in Molnar (2020). The average of the 5th percentile of the minimum autumn temperature ($\mu_{AutTx05}$) and the average number of days with heavy rain (μ_{h1r}) are the primary drivers of accelerated deterioration of concrete bridges, whereas the increasing average number of spring freeze-thaw cycles (μ_{ft2}) and variability of the 95th percentile of the minimum and maximum summer temperature ($\sigma_{SumTn95}$ and $\sigma_{SumTx95}$, respectively) can significantly hinder the deterioration of such bridges (Fig. 12a). On the other hand, increasing the number of bridge spans (n_s) can highly facilitate the deterioration of steel bridges whereas the high variability of frost season length (σ_{FFS}) and average 95th percentile of the maximum summer temperature ($\mu_{SumTx95}$) can result in a lower deterioration rate for steel bridges (Fig. 12b). These observations show that the geometric characteristics of bridges and climate conditions can together influence the deterioration of bridges, supporting the importance of developing climate-based infrastructure deterioration models.

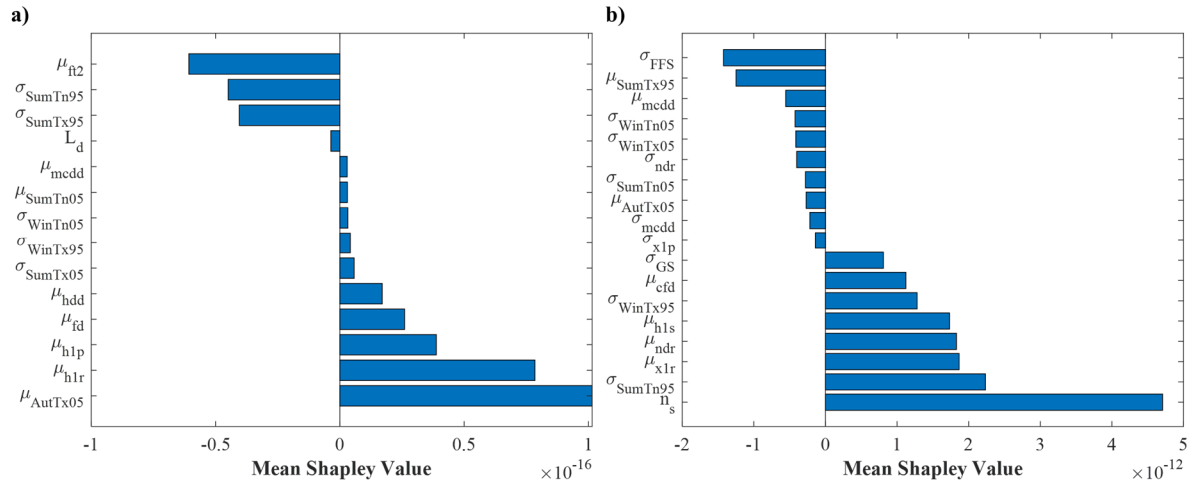

Fig. 12: The mean Shapely values for the inputs affecting the deterioration of (a) cast-in-place concrete frame and (b) weathering steel plat-I-girder bridges

4. CONCLUSION

Quantifying the infrastructure deterioration rate is key to estimate the corresponding lifespan, to design long-lasting infrastructure, to manage required rehabilitation plans, and to effectively allocate the available resources. However, the deterioration rate is influenced by the physical/chemical/functional infrastructure characteristics, as well as the ambient climate conditions. The latter influencing factor is of a particular importance due to the ongoing and expected climate change. In this respect, the present study proposes a framework that can be used to develop symbolic predictive models linking the deterioration rates of infrastructures to climate indices. To demonstrate its utility, the proposed framework was used to develop multigene genetic programming (MGGP)-based models for concrete and steel bridges in the province of Ontario, Canada. For the concrete bridges, the MGGP-based model effectively reproduced the actual deterioration rate values for the training subset with coefficient of determination (R^2) and root mean squared error (RMSE) values of 0.912 and 0.14, respectively. The model accuracy was slightly lower for the testing subset, with R^2 and RMSE values of 0.817 and 0.16, respectively. For the steel bridges, the accuracy of the MGGP-based model was nearly similar to that used for the concrete bridges for both the training (R^2 = 0.924 and RMSE=0.21) and testing subsets (R^2 = 0.909 and RMSE=0.25). A factor importance analysis revealed the minimum autumn temperature, minimum and maximum summer temperature, number of days with heavy rain, and number of spring freeze-thaw cycles can significantly impact the deterioration of concrete bridges, whereas the number of bridge spans, frost season length, and maximum summer temperature can highly control the deterioration of steel bridges. The results of the present study highlight the importance of incorporating the climate conditions when developing predictive models for infrastructure deterioration and support the efficiency of the proposed data-driven framework in developing these

integrated models. Such models can: 1) aid the designers and practitioners to efficiently determine the remaining lifespan of existing infrastructure, as well as the expected lifetime of those under design, considering the climate impacts; 2) assist the infrastructure asset managers to devise reliable repair strategies; and, 3) enable the policymakers to prepare effective asset management strategies considering future climate projections.

5. REFERENCES

Alabdulwahab, S., & Moon, B. (2020). Feature selection methods simultaneously improve the detection accuracy and model building time of machine learning classifiers. *Symmetry*, *12*(9), 1424.

Alzoor, F. S., Ezzeldin, M., Mohamed, M., & El-Dakhakhni, W. (2021). Prioritizing Bridge Rehabilitation Plans through Systemic Risk-Guided Classifications. Journal of Bridge Engineering, 26(7), 04021038.

ASCE. (2009). 2009 report card for America's infrastructure.

Assaad, R., & El-adaway, I. H. (2020a). Bridge infrastructure asset management system: Comparative computational machine learning approach for evaluating and predicting deck deterioration conditions. *Journal of Infrastructure Systems*, *26*(3), 04020032.

Babatunde, O. H., Armstrong, L., Leng, J., & Diepeveen, D. (2014). *A genetic algorithm-based feature selection*.

Bastidas-Arteaga, E., Schoefs, F., Stewart, M. G., & Wang, X. (2013). Influence of global warming on durability of corroding RC structures: A probabilistic approach. *Engineering Structures*, *51*, 259–266.

Berardi, L., Giustolisi, O., Kapelan, Z., & Savic, D. A. (2008). Development of pipe deterioration models for water distribution systems using EPR. Journal of Hydroinformatics, 10(2), 113–126.

Bolar, A., Tesfamariam, S., & Sadiq, R. (2014). Management of civil infrastructure systems: QFD-based approach. *Journal of Infrastructure Systems*, *20*(1), 04013009.

Braik, M. (2021). A Hybrid Multi-gene Genetic Programming with Capuchin Search Algorithm for Modeling a Nonlinear Challenge Problem: Modeling Industrial Winding Process, Case Study. *Neural Processing Letters*, 1–44.

Bu, G., Lee, J., Guan, H., Blumenstein, M., & Loo, Y.-C. (2014). Development of an integrated method for probabilistic bridge-deterioration modeling. *Journal of Performance of Constructed Facilities*, *28*(2), 330–340.

Bu, G. P., Son, J. B., Lee, J. H., Guan, H., Blumenstein, M., & Loo, Y. C. (2013). Typical deterministic and stochastic bridge deterioration modelling incorporating backward prediction model. *Journal of Civil Structural Health Monitoring*, *3*(2), 141–152.

Camacho, A. E. (2009). Adapting governance to climate change: managing uncertainty through a learning infrastructure. *Emory LJ*, *59*, 1.

Canadian Climate Data and Scenarios, 2019. Accessed 04/09/2021 https://climate-scenarios.canada.ca/?page=climate-indices-definition

Chang, C. M., Ortega, O., & Weidner, J. (2021). Integrating the Risk of Climate Change into Transportation Asset Management to Support Bridge Network-Level Decision-Making. *Journal of Infrastructure Systems*, *27*(1), 04020044.

Chang, M., Maguire, M., & Sun, Y. (2019). Stochastic modeling of bridge deterioration using classification tree and logistic regression. *Journal of Infrastructure Systems*, *25*(1), 04018041.

Cho, I. H. (2021). Initial Foundation for Predicting Individual Earthquake's Location and Magnitude by Using Glass-Box Physics Rule Learner. ArXiv Preprint ArXiv:2107.12915.

Chukwu, A. U., & Adepoju, K. A. (2012). On the power efficiency of artificial neural network (ANN) and the classical regression model. Progress in Applied Mathematics, 3(2), 28–34.

Chudasama, C., Shah, S. M., & Panchal, M. (2011). Comparison of parents selection methods of genetic algorithm for TSP. *International Conference on Computer Communication and Networks CSI-COMNET-2011, Proceedings*, 85–87.

Cuevas, A., Febrero, M., & Fraiman, R. (2002). Linear functional regression: the case of fixed design and functional response. Canadian Journal of Statistics, 30(2), 285–300.

Cui, X., Zhang, N., Li, S., Zhang, J., & Tang, W. (2016). Deterioration of soil-cement piles in a saltwater region and its influence on the settlement of composite foundations. *Journal of Performance of Constructed Facilities*, *30*(1), 04014195.

Darwin, Charles, and Leonard Kebler. On the origin of species by means of natural selection, or The preservation of favoured races in the struggle for life. London: J. Murray, 1859.

De Smith, M. J., Goodchild, M. F., & Longley, P. (2007). *Geospatial analysis: a comprehensive guide to principles, techniques and software tools*. Troubador publishing ltd.

Derrible, S., Chester, M., & Guikema, S. (2020). *Infrastructure Resilience to Climate Change*. American Society of Civil Engineers.

Duch, W. (2006). Filter methods. In *Feature Extraction* (pp. 89–117). Springer.

Ekart, A., & Nemeth, S. Z. (2001). Selection based on the pareto nondomination criterion for controlling code growth in genetic programming. *Genetic Programming and Evolvable Machines*, *2*(1), 61–73.

lmansouri, O., Almhroog, A., & Badi, I. (2020). Urban transportation in Libya: An overview. Transportation Research Interdisciplinary Perspectives, 8, 100161.

Gandomi, A. H., & Alavi, A. H. (2012). A new multi-gene genetic programming approach to nonlinear system modeling. Part I: materials and structural engineering problems. *Neural Computing and Applications*, *21*(1), 171–187.

Gandomi, A. H., Sajedi, S., Kiani, B., & Huang, Q. (2016). Genetic programming for experimental big data mining: A case study on concrete creep formulation. *Automation in Construction*, *70*, 89–97.

Gondia, A., Ezzeldin, M., & El-Dakhakhni, W. (2020). Mechanics-guided genetic programming expression for shear-strength prediction of squat reinforced concrete walls with boundary elements. *Journal of Structural Engineering*, *146*(11), 04020223.

Grosman, B., & Lewin, D. R. (2002). Automated nonlinear model predictive control using genetic programming. *Computers & Chemical Engineering*, *26*(4–5), 631–640.

Inkoom, S., Sobanjo, J., & Chicken, E. (2021). Performance Assessment of Deteriorating Bridge Channels in the Presence of Hurricane Failures: The Competing Risks Scenario. *Journal of Infrastructure Systems*, *27*(1), 04020041.

IPCC, 2021: Climate Change 2021: The Physical Science Basis. Contribution of Working Group I to the Sixth Assessment Report of the Intergovernmental Panel on Climate Change [Masson Delmotte e. al.] Cambridge University Press. In Press.

Ishida, T., Fang, J., Fathalla, E., & Furukawa, T. (2021). Data driven maintenance cycle focusing on deterioration mechanism of road bridge RC decks. In *Bridge Maintenance, Safety, Management, Life-Cycle Sustainability and Innovations* (pp. 1204–1210). CRC Press.

Jeong, H., Kim, H., Kim, K., & Kim, H. (2017). Prediction of flexible pavement deterioration in relation to climate change using fuzzy logic. *Journal of Infrastructure Systems*, *23*(4), 04017008.

Jiang, Y., Saito, M., & Sinha, K. C. (1988). *Bridge performance prediction model using the Markov chain* (Issue 1180).

Jiang, Y., & Sinha, K. C. (1989). Bridge service life prediction model using the Markov chain. *Transportation Research Record*, *1223*(1), 24–30.

Khelifa, A., Garrow, L. A., Higgins, M. J., & Meyer, M. D. (2013). Impacts of climate change on scour-vulnerable bridges: Assessment based on HYRISK. *Journal of Infrastructure Systems*, *19*(2), 138–146.

Koljonen, J., & Alander, J. T. (2006). Effects of population size and relative elitism on optimization speed and reliability of genetic algorithms. *Proceedings of the Ninth Scandinavian Conference on Artificial Intelligence (SCAI 2006)*, 54–60.

Koza, J. R. (1994). Genetic programming as a means for programming computers by natural selection. *Statistics and Computing*, *4*(2), 87–112.

Le, N., Xuan, H. N., Brabazon, A., & Thi, T. P. (2016). Complexity measures in Genetic Programming learning: A brief review. *2016 IEEE Congress on Evolutionary Computation (CEC)*, 2409–2416.

Liu, L., Yang, D. Y., & Frangopol, D. M. (2020). Network-level risk-based framework for optimal bridge adaptation management considering scour and climate change. Journal of Infrastructure Systems, 26(1), 04019037.

Lounis, Z., & Madanat, S. M. (2002). Integrating mechanistic and statistical deterioration models for effective bridge management. In *Applications of Advanced Technologies in Transportation (2002)* (pp. 513–520).

Mekis, E., & Vincent, L. A. (2008). Changes in daily and extreme temperature and precipitation indices related to droughts in Canada. *17th Conference on Applied Climatology, Whistler, BC, Canada*.

Mehr, A. D., & Safari, M. J. S. (2020). Multiple genetic programming: a new approach to improve genetic-based month ahead rainfall forecasts. Environmental Monitoring and Assessment, 192(1), 1–12.

Melchers, R. E. (2006). Recent progress in the modeling of corrosion of structural steel immersed in seawaters. *Journal of Infrastructure Systems*, *12*(3), 154–162.

Mirza, S. (2006). Durability and sustainability of infrastructure—A state-of-the-art report. *Canadian Journal of Civil Engineering*, *33*(6), 639–649.

Molnar, C. (2020). Interpretable machine learning. Lulu. com.

Myers, R. H., & Myers, R. H. (1990). Classical and modern regression with applications (Vol. 2). Duxbury press Belmont, CA.

Nickless, K., & Atadero, R. A. (2018). Mechanistic deterioration modeling for bridge design and management. *Journal of Bridge Engineering*, *23*(5), 04018018.

Oliver, M. A., & Webster, R. (1990). Kriging: a method of interpolation for geographical information systems. *International Journal of Geographical Information System*, *4*(3), 313–332.

Peng, L., & Stewart, M. G. (2016). Climate change and corrosion damage risks for reinforced concrete infrastructure in China. *Structure and Infrastructure Engineering*, *12*(4), 499–516.

Peralta, B., & Soto, A. (2014). Embedded local feature selection within mixture of experts. *Information Sciences*, *269*, 176–187.

Piryonesi, S. M., & El-Diraby, T. (2021). Climate change impact on infrastructure: A machine learning solution for predicting pavement condition index. *Construction and Building Materials*, *306*, 124905.

Pistore, L., Pernigotto, G., Cappelletti, F., Gasparella, A., & Romagnoni, P. (2019). A stepwise approach integrating feature selection, regression techniques and cluster analysis to identify primary retrofit interventions on large stocks of buildings. *Sustainable Cities and Society*, *47*, 101438.

Rahmstorf, S., & Coumou, D. (2011). Increase of extreme events in a warming world. *Proceedings of the National Academy of Sciences*, *108*(44), 17905–17909.

Ring, M. J., Lindner, D., Cross, E. F., & Schlesinger, M. E. (2012). Causes of the global warming observed since the 19th century. *Atmospheric and Climate Sciences*, *2*(04), 401.

Rylander, S. G. B., & Gotshall, B. (2002). Optimal population size and the genetic algorithm. *Population*, *100*(400), 900.

Scheffran, J., & Battaglini, A. (2011). Climate and conflicts: the security risks of global warming. *Regional Environmental Change*, *11*(1), 27–39.

Searson, D. P., Leahy, D. E., & Willis, M. J. (2010). GPTIPS: an open source genetic programming toolbox for multigene symbolic regression. *Proceedings of the International Multiconference of Engineers and Computer Scientists*, *1*, 77–80.

Shen, J., & Jimenez, R. (2018). Predicting the shear strength parameters of sandstone using genetic programming. *Bulletin of Engineering Geology and the Environment*, *77*(4), 1647–1662.

Shen, Y., Goodall, J. L., & Chase, S. B. (2019). Condition State–Based Civil Infrastructure Deterioration Model on a Structure System Level. *Journal of Infrastructure Systems*, *25*(1), 04018042.

Sillmann, J., & Roeckner, E. (2008). Indices for extreme events in projections of anthropogenic climate change. *Climatic Change*, *86*(1), 83–104.

Stevens, N. A., Lydon, M., Campbell, K., Neeson, T., Marshall, A., & Taylor, S. E. (2020). *Conversion Of Legacy Inspection Data To Bridge Condition Index (BCI) To Establish Baseline Deterioration Condition History For Predictive Maintenance Models.*

Stewart, M. G., Wang, X., & Nguyen, M. N. (2011). Climate change impact and risks of concrete infrastructure deterioration. *Engineering Structures*, *33*(4), 1326–1337.

Stewart, M. G., Wang, X., & Nguyen, M. N. (2012). Climate change adaptation for corrosion control of concrete infrastructure. *Structural Safety*, *35*, 29–39.

Strauss, A., Wendner, R., Bergmeister, K., & Costa, C. (2013). Numerically and experimentally based reliability assessment of a concrete bridge subjected to chloride-induced deterioration. *Journal of Infrastructure Systems*, *19*(2), 166–175.

Sultana, M., Chai, G., Chowdhury, S., Martin, T., Anissimov, Y., & Rahman, A. (2018). Rutting and roughness of flood-affected pavements: Literature review and deterioration models. *Journal of Infrastructure Systems*, *24*(2), 04018006.

Taha, I. A., & Ghosh, J. (1999). Symbolic interpretation of artificial neural networks. IEEE Transactions on Knowledge and Data Engineering, 11(3), 448–463.

Tari, Y. H., Shamsabadi, S. S., Birken, R., & Wang, M. (2015). Deterioration modeling for condition assessment of flexible pavements considering extreme weather events. Structural Health Monitoring and Inspection of Advanced Materials, Aerospace, and Civil Infrastructure 2015, 9437, 943721.

Underwood, B. S., Mascaro, G., Chester, M. v, Fraser, A., Lopez-Cantu, T., & Samaras, C. (2020). Past and present design practices and uncertainty in climate projections are challenges for designing infrastructure to future conditions. *Journal of Infrastructure Systems*, *26*(3), 04020026.

Wellalage, N. K. W., Zhang, T., & Dwight, R. (2015). Calibrating Markov chain–based deterioration models for predicting future conditions of railway bridge elements. *Journal of Bridge Engineering*, *20*(2), 04014060.

Yang, D. Y., & Frangopol, D. M. (2020). Risk-based vulnerability analysis of deteriorating coastal bridges under hurricanes considering deep uncertainty of climatic and socioeconomic changes. *ASCE-ASME Journal of Risk and Uncertainty in Engineering Systems, Part A: Civil Engineering*, *6*(3), 04020032.

Yegnanarayana, B. (2009). Artificial neural networks. PHI Learning Pvt. Ltd.

Yin, X., Chen, Y., Bouferguene, A., & Al-Hussein, M. (2020). Data-driven bi-level sewer pipe deterioration model: Design and analysis. Automation in Construction, 116, 103181.

Yosri, A., Elleathy, Y., Hassini, S., & El-Dakhakhni, W. (2021). Genetic Algorithm-Markovian Model for Predictive Bridge Asset Management. *Journal of Bridge Engineering*, *26*(8), 04021052.

Zhang, W., & Durango-Cohen, P. L. (2014). Explaining heterogeneity in pavement deterioration: Clusterwise linear regression model. *Journal of Infrastructure Systems*, *20*(2), 04014005.

Zhou, S., Yang, Y., Ng, S. T., Xu, J. F., & Li, D. (2020). Integrating data-driven and physics-based approaches to characterize failures of interdependent infrastructures. International Journal of Critical Infrastructure Protection, 31, 100391.